International Journal of Engineering Research & Technology (IJERT)
ISSN: 2278-0181
Vol. 3 Issue 8, August - 2014

Meta-Analysis of Corrosion Behaviour

Jeegar Joshi
Deputy Manager, Essar Steel India Limited,
Hazira, Gujarat.

Dhruval Shah
Deputy Manager, Essar Steel India Limited,
Hazira, Gujarat.

Abstract— Non Renewable energy resources (Coal, Natural gas, oil and bio-fuel) still accounts for major sources of power generation to satisfy the growing power needs of nations around the world. According to International Energy Agency (IEA) the demand in primary energy will increase by up to 49% by 2035.The power industry suffers huge annual losses in the form of maintenance repairs resulting from the super heater corrosion. There is a huge downtime involved due to super heater tube failures.These tube failures are almost exclusively caused by fireside tube metal wastage driven by complicated mechanisms of corrosion in combination with local erosion. The corrosion is caused by salts in the slag that deposits on the boiler tubes, coupled with high temperatures of flue gas going through the boiler.In this study, we have done a meta-analysis (Analysis of analysis) of various research published in the area and used the results to predict the corrosion rate (For base metal and Weld Separately) - for different boiler environments and temperature conditions. In the study, 4 samples(two of base metal and two of weld) were taken of T92 chrome- molybdenum alloy (Ultra super-critical boiler material), two of the samples (one of base metal and one of weld) were heated at 650 degree Celsius and the other two samples (one of base and one of weld) at 750 degree Celsius. The samples at each of the temperatures were put in two different salts (Salt-I and Salt-II) thereby simulating the actual boiler working conditions. Each sample was heated for 5 hours then cooled to room temperature and weighed. The process was repeated for 10 cycles for 50 hours.Upon completion of the corrosion kinetics study, the specimens were examined by optical metallography and a scanning electron microscope (SEM) equipped with energy–dispersive X–ray analyser (EDAX). Optical examination of cross sections of exposed specimens, and analyses with the SEM, were used to identify the morphological features of corrosion product phases in the scale layers and to establish the thickness of scales. The fundamental idea for such an analysis is that if the corrosion could be reliably predicted, new power plants could be designed accordingly, and knowledge of fuel selection and determination of process conditions could be utilized to minimize the super heater corrosion. This result will help reduce some burden on the power industries and will also help to minimise pollution.

Keywords: Heat Affected Zone (HAZ), Ultra-Super Critical Boiler (USC), Scanning electron Microscope (SEM), Energy dispersive X-ray Analyser (EDAX), Super heater.

1. INTRODUCTION

Ferritic steels, containing chromium and molybdenum are well known for their excellent mechanical properties combining high temperature strength and creep resistance with high thermal fatigue life, as well as with good thermal conductivity, weldability, and resistance to corrosion and graphitisation. Because of these characteristics this type of steels have attracted special interest for application in industrial processes related to carbochemistry, oil refining, carbon gasification and energy generation in thermal power plants, where components like, heat exchangers, boilers and pipes operate at high temperatures and pressures for long periods of time[1].

Power generation industries are very important for both developed and a developing country since electrical energy has become a fundamental requirement for human beings. The generation of increasing amounts of electricity while simultaneously reducing environmental emissions has become a goal for the power generation industry worldwide. According to international energy agency (IEA) the demand in primary energy will increase by up to 49% by 2035 [2]. The power generation industry around the world is under tremendous pressure to generate a sufficient amount of power which is sustainable, affordable and reliable; and meet the industrial, transport, and domestic requirements. Some of the different sources used to generate electrical energy are: nuclear, solar, wind, hydro, bio-fuel, waste, fuel cell. However, fossil fuels (coal, oil and natural gas) are the main sources used within the power generation industry, and conventional steam turbine power plants are still widely used across the globe as the main source of power generation. Figure 1-1 illustrates the world electric generation from different fuel sources.

Superheater corrosion causes vast annual losses to the power companies. If the corrosion could be reliably predicted, new power plants could be designed accordingly, and knowledge of fuel selection and determination of process conditions could be utilized to minimize of superheater corrosion. The material loss in superheaters is one of the most expensive phenomena as far as the maintenance costs of commercial boilers are concerned.

Superheater corrosion is a common reason for boiler shutdown. A shutdown and consequent superheater repair significantly increase the operating costs of a boiler.

Fireside corrosion is often a very complicated process. Metal loss in a superheater can occur due to oxidation, sulfidation, erosion-corrosion, or a combination of these. Chlorine-containing deposits may also be one of the crucial factors
causing metal loss.

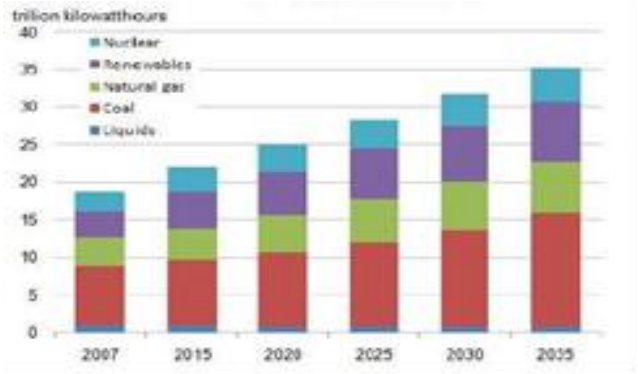

Figure 1-1: World net electricitry generation by fuel [2]

1.2 OXIDATION OF MATERIAL IN BOILER PLANTS

The most common metal degradation mechanism encountered in combustion is oxidation. Oxidation takes place when the oxygen in the flue gas gets in contact with the superheater steel surface. Due to the need for elevated strength at high temperatures, the steels used in superheaters are often chromium and/or nickel containing alloys.The Oxidation of the alloy surface creates a protective iron or chromium oxide layer which prevents diffusion of oxygen. Because of the decreased diffusion, the oxidation rate slows down, and a stable oxide layer is formed on the steel surface.

This type of oxidation is called selective, and the mechanism is widely used for protection against corrosion. The oxidation rate constants depend on the metal, the temperature, and the diffusion coefficient of oxygen through the oxide layer. If the diffusion rate through the oxide layer is high, the oxide forms no protection against further oxidation.

1.3 SULFIDATION OF MATERIAL IN BOILER PLANTS

Sulfur corrosion, often referred to as sulfidation, is a very common phenomenon in coal combustion, but it can also occur with other fuels. In the combustion process, the sulfur in fuel reacts with oxygen in the combustion air forming SO2, and, if the residence time and O2 content are sufficient, it formsalso SO3. The initial sulfidation reaction seldom continues so as to result in internal sulfidation of the metal.

1.4 CHLORINE-INDUCED CORROSION IN BOILER PLANT

Chlorine-induced corrosion is a common corrosion type in waste combustion. This type of corrosion can also take place in combustion of other chlorine-containing fuels, for example biofuels and high-chlorine coals. Chlorine corrosion is often accelerated by alkaline components in the fuel. At low temperatures, chlorine corrosion can take place as hydrochloric acid corrosion, but in the case of superheater corrosion, the mechanism is initiated when the fuel contains sufficient amounts of chlorine, and the superheater tube temperature is sufficient for chlorides to form molten eutectics.

Fireside metal wastage in conventional coal-fired boilers can occur by gas- phase oxidation or deposit-induced liquid-phase corrosion. The former can be minimized by using materials that are resistant to oxidation at the service temperatures of interest. On the other hand, deposit-induced corrosion of materials is an accelerated type of attack, influenced by the vaporization and condensation of small amounts of impurities such as sodium, potassium, sulfur, chlorine, and vanadium (or their compounds) that are present in the coal feedstock.

At the temperatures of interest in advanced combustion systems, Mixtures of alkali sulfates, along with alkali chlorides, will dominate the fireside deposit, and viable structural alloys must be resistant to attack by such deposits. The temperature regimes in which this corrosion occurs are summarized in Figure 2.

The effect of hot corrosion on the welds also leads to its failure. The oxide formed due to oxidation, degrades the weld property. The corrosion property of weld is different from the base material. So our study is concentrated on observing the corrosion rate of the base material and weld differently. In present investigation, T92 ferritic stainless steel base and TIG welded cut sample is used for the hot corrosion test. After no. of heating cycle weight loss is measured and the macro and micro images were taken.

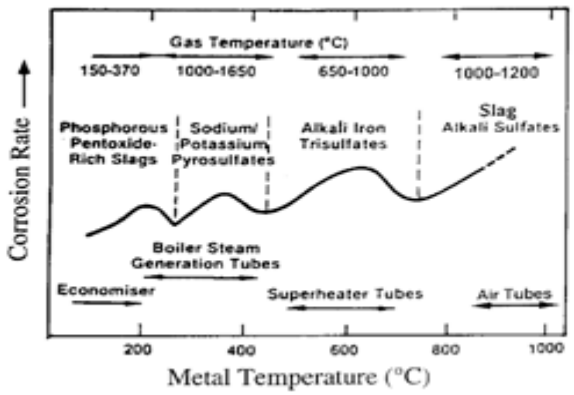

Figure 2: Regimes of fireside corrosion in coal-fired boilers

1.5 OBJECTIVES

To evaluate the weight change of the base and weld metal, to examine macro and micro structural changes after the heating cycles and to study the corroded surface morphology through SEM and oxide formation through EDAX.

2.0 EXPERIMENTAL TECHNIQUE

2.1 BASE MATERIAL

T92 is an ASTM A213 Grade ferritic stainless steel which is used for the present study. It is an ultra super critical boiler material, which can operate at high temperature of 650°C. It has the high elevated temperature strength and excellent creep strength. It has the good resistance to high temperature corrosion and steam oxidation. It shows good resistance to thermal fatigue superior to austenitic stainless steels. The chemical composition for the same is listed below in table 3.1.

C%	Cr%	Ni%	W%	Si%	Nb%	Mo%	N%	Mn%	P%	S%	B%	Fe%
0.13	9.5	0.4	2	0.5	0.09	0.6	0.07	0.6	0.02	0.01	0.006	Bal.

Table 3.1 Chemical composition of T92 material

2.2 WELDING PARAMETERS

The current, voltage and the variation of the WFR (wire feed rate) can be measured by the digital display on the power source. During the welding process, the power source characteristics like voltage, current, WFR, standoff distance of TIG process have been studied and tabulated. The TIG welding parameters are tabulated in table 3.2.

parameter	value
Process	GTAW
Current	75A-220A
Voltage	15.5V-16.5V
Filler wire feed rate	4m/min
Filler wire	ER90S-G(92)
Welding position	1G rotating
Joint	V-groove Butt joint
Electrode	Th-W
Gas flow rate	18Lpm
Shielding gas	90%Ar+10%CO_2
No. of pass	2
Preheat temperature	220°C
Post-heat temperature	760°C for 30min.

Table 3.2: TIG welding parameter

2.3 MACRO AND MICRO IMAGE OF WELDMENT

The weldment cut from the tube were cold mounted to see the macro and micro images to study the micro structure of the base, weld and the HAZ (heat affected zone) of the weldment. After suitable surface preparation the images are shown in the figures shown below.

(a) (b)

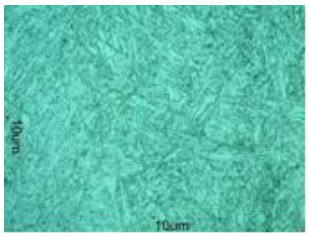

(c)

Figure 3.3 at 500X (a) Base Metal, (b) HAZ, and (c) Weld

2.4 TUBULAR RESISTANCE FURNACE

The schematic diagram of the experimental setup used for the isothermal corrosion tests is shown in Figure. 3.4. The experiments were conducted in a horizontal resistance-heated furnace that contained a 55-mm-i.d. x 3-mm-wall alumina reaction tube (make: v. b. ceramic consultant, Chennai, India). The temperature was measured by a thermocouple inserted into an alumina thermo well that was fed through an opening in the flange of the reaction chamber.

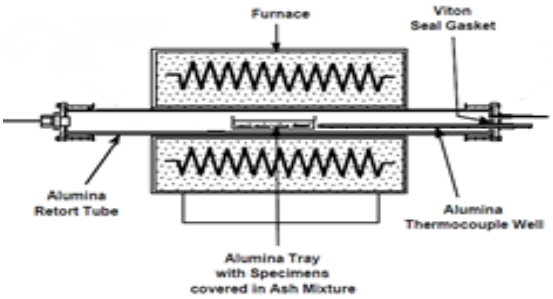

Figure 3.4 Schematic diagram of furnace assembly

2.5 PREPARING SAMPLES

The eight samples (4 Base and 4 Weld), in the form of cuboid. They were polished to some extent, identified by letters stamped on it and were thoroughly degreased in clean acetone, rinsed in water and dried.

Sample Name: T92 Base, Base sample Length: 13mm, Base sample width: 5mm, Base sample thickness: 5mm.

Sample Name: T92 Weld, Weld sample length: 11mm, weld sample width: 7mm, weld sample thickness: 6mm.

2.6 MIXTURE PREPARATION

Two salts used to create the boiler simulating condition contain ash, Na2SO4 and V2O5 (salt-I) & the ash, alkali sulfate (Na2SO4), KCl and NaCl (salt-II) in the weight proportion of 75:10:15 & 85:5:5:5, in the form of powder is prepared. This proportion melts and makes sludge at high temperature, which is further stick to the material surface for oxidizing. Proportion of the salts is given in the below table 3.3 and table 3.4.

Ash	Na_2SO_4	V_2O_5
75	10	15

Table 3.3 Weight % for salt-1

Ash	Na2SO4	KCl	NaCl
85	5	5	5

Table 3.4 Weight % for salt-2

2.7 EXPERIMENTAL PROCEDURE

1. The samples for the experiment cut from the welded tube of T92 material, in which the four samples were from the base material and the rest four were from the weld area. The cut samples were filed and polished with SiC paper to get even uniform surface and to let the salt to stick with the surface of the sample. All the samples were washed with water dried with dryer to remove dust and other particle and then kept for ultrasonic cleaning with acetone to remove other left particle and the moisture from the surface and dried using dryer.

2. The alumina boat to hold the different samples with salt is also rinsed with the water and with acetone ultrasonically cleaned to make it free from any water particle and moisture and dried using dryer.

3. Now the base and weld sample placed into the alumina boat. The amount of the salt to be spread over the sample is taken as the 3.5 times the surface area (in mm2) of the sample, in milligram.
(Surface Area) of Base/Weld = 2(LxW+WxT+TxL)
(SA) of B = 2(13x5+5x5+5x13) = 310 mm2
(SA) of W = 2(11x7+7x6+6x11) = 370 mm2
Weight of salt = [3.5x2(LxW+WxT+TxL)] milligram.
Where L= length, W= width & T= thickness of sample.
For base weight of salt were taken as
S of B = [3.5x2(13x5+5x5+5x13)] milligram = 1080mg = 1.08gram.
For weld weight of salt were taken as
S of W = [3.5x2(11x7+7x6+6x11)] = 1295mg = 1.295gram.

4. After calculating the amount of salts to be put on the samples, the alumina boat with sample and salt were sprinkled with little drop of water to settle down the salt into the boat with the sample. The boats were placed inside the tubular furnace for removing the water particle and moisture left in the boat.

5. The samples with salt kept inside the tubular furnace at 800°C for 2 hours of soaking to make it completely free of any kind of moisture from the salt in boat. After 2 hours of soaking the samples were let cool down to room temperature and then initial weight of the boat along with salt and sample were taken.

6. After each 5 hours of soaking time in tubular furnace the sample were cooled to room temperature and the weight was taken with the electronic weighing machine. Further the procedure were repeated up to 10 consecutive cycle, 5 hours of each cycle, for total 50 hours of soaking time.

7. The whole procedure were done for the two samples i.e. Base and Weld for salt-I at a temperature of 650°C, in two different alumina boat. After completing total 50 hours of soaking cycle for the previous samples, the new Base and Weld kept with the salt-II for 650°C.

8. The soaking cycles were completed for two different salts for the different base and weld for a particular temperature of 650°C. The same procedures were again repeated for the temperature of 750°C for two different salts.

9. The weight change data obtain after each cycle of soaking time is noted down and comparative graphs were plotted for all variables i.e. Base and Weld, two different salts and two different temperatures.

10. Upon completion of the corrosion kinetics experiments, the specimens were examined by optical metallography and a scanning electron microscope (SEM) equipped with energy–dispersive X–ray analyzer. Optical examination of cross sections of exposed specimens, and analyses with the SEM, were used to identify the morphological features of corrosion product phases in the scale layers and to establish the thickness of scales.

2.8 HARDNESS TEST

Hardness value of base metal, heat affected zone and weld metal is calculated using Vickers hardness method at load at 5kg. The Vickers hardness test is an indentation hardness test in which a square based pyramidal diamond indenter with specified face angles is forced into the surface of the material. The Vickers hardness number is related to the applied load and the surface area of the permanent impression.

Hardness measurement provides indications of metallurgical changes caused by welding, metallurgical variation and abrupt microstructural discontinuities in weld joints, brittleness and relative sensitivity to cracking under structural loads. The equipment is already calibrated hence the hardness value is obtained directly by specifying the edges of the indentation. The figure for the Vickers hardness test is given in the figure: 3.5.

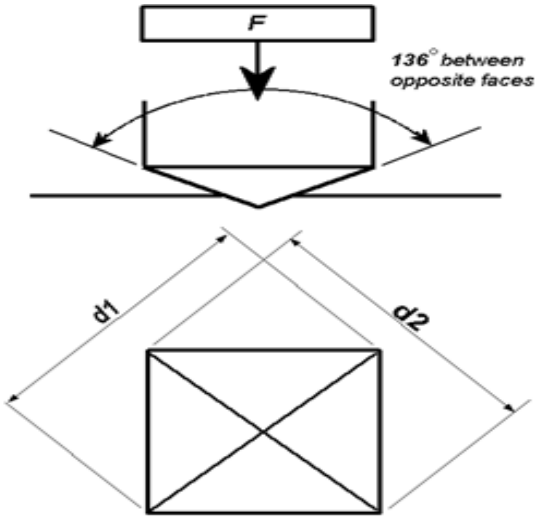

Figure 3.5: Indendation schematic diagram on Vickers hardness testing machine

3.0 RESULTS AND DISCUSSION

3.1 STUDIES ON CORROSION RATE

The corrosion rate for the base and weld for two different variables i. e. temperature and salt is observed, in which samples were exposed to the given variables for 10 no. of heating cycles (5 hours for each cycle), total of 50 hours. From the figure 4.1 we can observe the base and weld, for a particular temperature for two different salts showing the different variation in weight change per cm square of surface area of base metal for different time intervals.

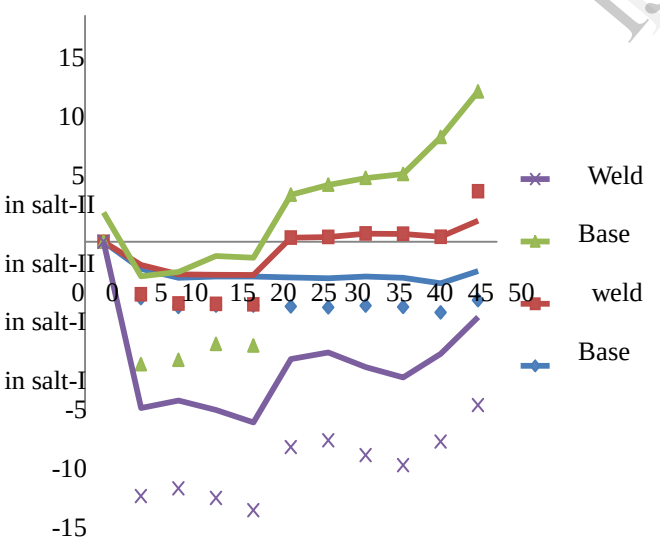

Y-axis: Weight change in mg/cm2, X-axis: soaking time (hrs)

Figure 4.1 corrosion rates of base and weld at 650°C

In the graph it is showing that the base in salt-I having almost moderate weight loss but in salt-II after some intervals of heating cycle it is showing a weight loss and then a weight gain. Almost same phenomenon occurs for weld in salt-I. But weld in salt-II is showing increase and decrease in weight lost. The salt-II contains NaCl, which accelerate the corroding process. In this temperature of 650°C, oxidation taking places more for base than the weld for salt-II. But in salt-I the oxidation of weld is taking place more than the base.

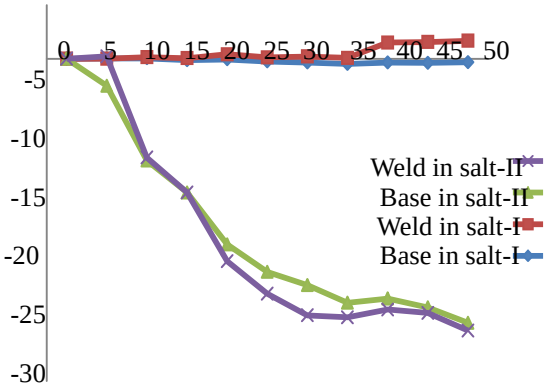

Y-axis: Weight change in mg/cm2, X-axis: soaking time (hrs)

Figure 4.2: Corrosion rates of base and weld at 750°C

At temperature of 750°C the corrosion rate graphs have shown by the below figures. As we can observe from the graph in figure 4.2 that oxidation of base in salt-I is almost very less compare to the weld and the in salt-II the oxidation or weight loss is decreasing drastically. The weight loss in salt-II for both weld and base is almost same.

For particular salt-I the comparative graphs have shown by The below figures. As can be noted, the oxidation of base metal at two temperatures of 750°C and 650°C is having a small difference, salt-I at temperature of 750°C the weld is showing higher oxidation as compare to at temperature of 650°C.

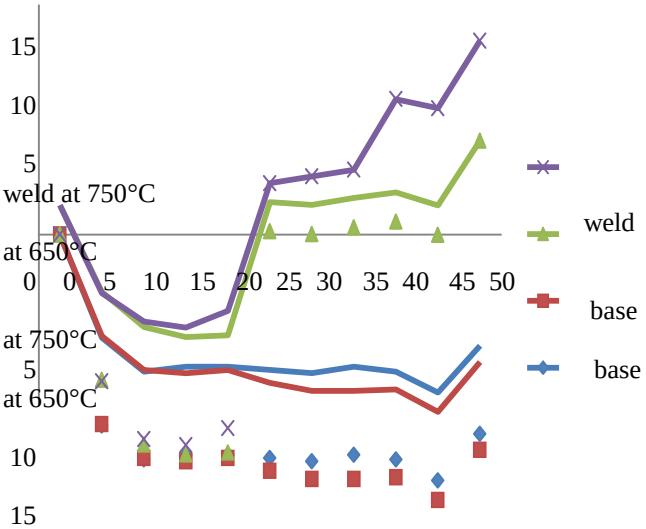

Y-axis: Weight change in mg/cm2, X-axis: soaking time (hrs)

Figure 4.3: Corrosion rates for base and welds at different temperatures for salt-I

In salt-II the base metal weight loss at temperature of 750°C is very high comparatively to at temperature of 650°C. For weld at temperature 650°C weight loss is little less than weight loss at temperature at 750°C. The graph in figure 4.3 shows the comparative weight change in salt-I for base and weld at different temperature of 650°C and 750°C.

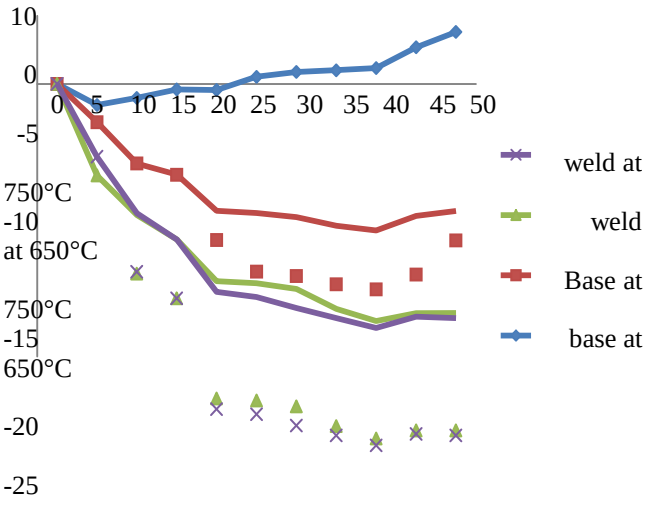

Y-axis: Weight change in mg/cm2, X-axis: soaking time (hrs)

Figure 4.4: corrosion rates for base and weld at different temperatures for salt-II

The weight loss for base metal for both temperatures is higher than the weld. From the graph in figure 4.4 which shows the comparative weight loss of the base and weld in salt-II, it is observed that the weight gain for the base is increasing for base at temperature of 650°C, which shows the oxidation of base is increasing with the time interval. For other base metal and two weld metal the weight loss is increases gradually for the two temperatures**.**

3.2 MACRO IMAGE STUDY

From the macro study we can observe that at temperature of 650°C in salt-I the pitting corrosion occurred on base and weld, where the base metal is having an adhered oxide layer and the on the weld a peeled off surface surface is coming to picture**.**

Also it is observed that at temperature of 750°C the base is attacked locally and the protective oxide layer is peeled off at some points, where in weld the severity is little high then the base. In salt-II the oxide layer is very thick and also pitting corrosion took place on the base. For the weld at this temperature the larger area, compare to base got peeled off which shows the intensity of corrosion on it.

3.3 SEM AND EDAX ANALYSIS

The given figures below shows the SEM images of the base and weld samples before and after the corrosion test, their respective EDAX graph and the element present in the particular area of the surface, in percentile of that area.

In the EDAX graph the peaks shows the elements present in there. From the graph, the higher peak shows the higher percentile of the element.

From the given figure 4.6 which shows the surface of the sample after the corrosion test, we can see that the elements like O, Fe and Cr are predominating. It is indicating that the oxides of Fe and Cr present on the surface. These oxides of Fe and Cr act as a protective layer to some extent for the metal surfaces exposed to corroding environment.

From figure 4.6 onward almost in all SEM images we can observe that the corrosion which is occurred is localized on the surfaces which is called pitting corrosion.

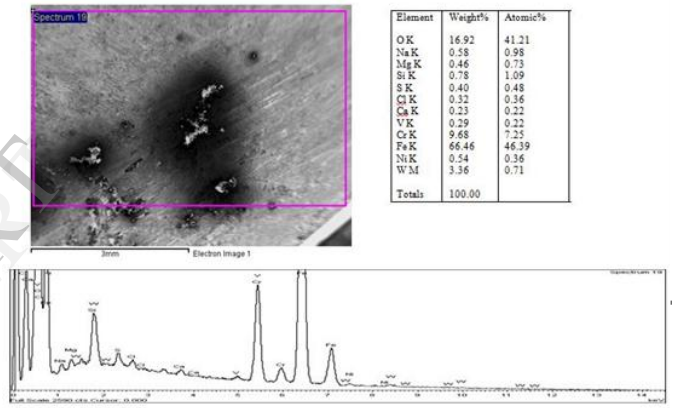

Figure 4.5: SEM image, element available in shown area and EDAX analysis (wt%) or base metal before corrosion

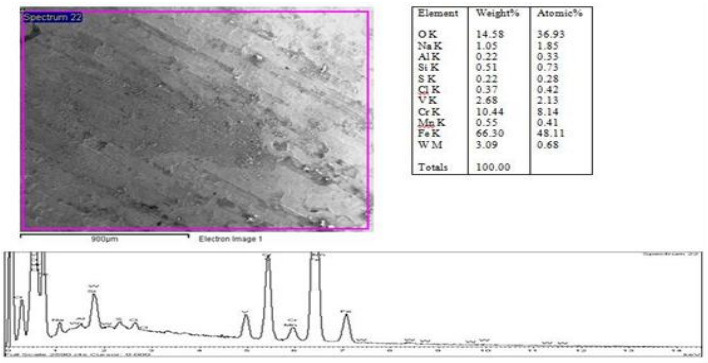

Figure 4.6: SEM image, element available in shown area and EDAX analysis (wt%) for base metal after corrosion in salt-I, at 650°C

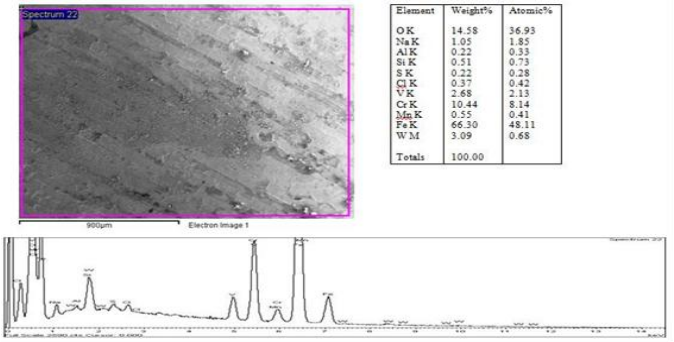

Figure 4.7: SEM image, element available in shown area and EDAX analysis (wt%) for base metal after corrosion in salt-II at 650°C

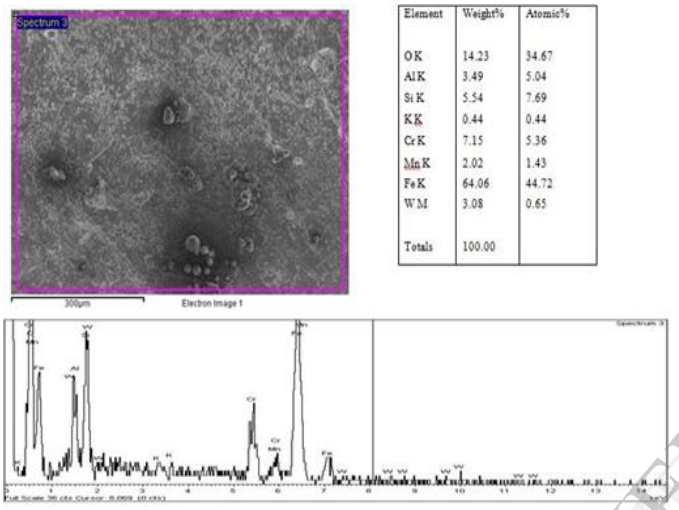

Figure 4.8: SEM image, element available in shown area and EDAX graph for analysis (wt%) metal after corrosion in salt-I, at 750°C

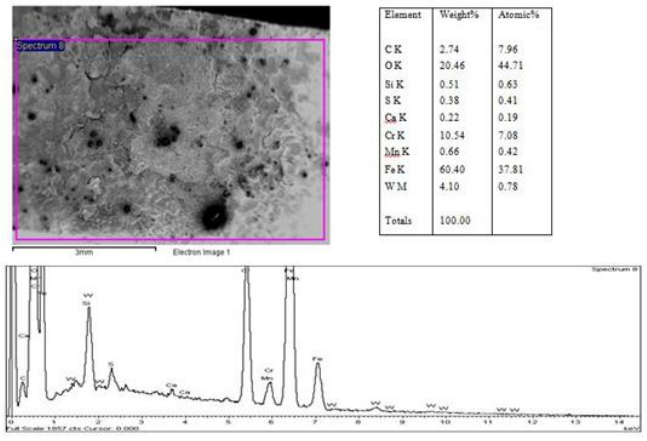

Figure 4.9: SEM image, element available in shown area and EDAX analysis (wt %) for base metal after corrosion in salt-II, at 750°C

From the graph in figure 4.6 it is clearly showing the oxide of Fe is high as compare to Cr. The weld metal is having the Fe oxide will protect for some time interval after which it may deplete from the surface due to temperature and the environment it exposed of. As we can see from the figure 4.4 the oxidation of weld is increasing after some time interval.

All composition occurred on the surface of the base and weld is oxides of Fe, Cr and few amount of W, as we can see from the graph.

4.0 CONCLUSION

The fireside corrosion test of the T92 material and its weldment is carried out in simulated boiler plant condition for two types of salt (environment) and for two temperatures of 650°C & 750°C, for 10 no. of heating cycle each of 5 hours, total of 50 hours. Based on the study following conclusion were made.

1. The type of corrosion occurs for base and weld is pitting type corrosion as we have observed from the macro and SEM images.
2. From the EDAX graph we have observed the presence of elements and oxides, which is found on the base and weld surface before and after corrosion test. Mainly the oxides of Fe and Cr are dominating on the surfaces of samples after the test.
3. For a particular temperature of 650°C the weight loss of base in salt-I is increases. Where in salt-II base shows fast Increment in weight gain after 25 hours of heating.
4. For a particular temperature of 650°C the weight loss of Weld in salt-I increases and after 25 hours of heating it Slowly decreases that means weight gain increases. Where In salt-II the weight loss increased drastically and little variation occurs in it.
5. For a particular temperature of 750°C the weight loss for base in salt-I is almost constant, where in salt-II the weight loss is drastically increases.
6. For a particular temperature of 750°C the weight gain of weld is almost negligible upto 30 hours of heating cycle. After it increases slowly upto 40 hours of heating cycle and then become constant from 40 to 50 hours of heating cycle.

REFERENCES

1. Dinesh Gond, Vikas Chawla, D. Puri, S. Prakash Oxidation Studies of T-91 and T-22 Boiler Steels in Air at 900°C, Vol. 9, No.8, pp.749-761, 2010.
2. K. Natesan, A. Purohit and D. L. Rink, Fireside Corrosion of Alloys for Combustion Power Plants
3. Zhuyao Zhang, Graham Holloway, Adam Marshall, Metrode Products Limited, UK, Properties of T/P92 Steelweld Metals for Ultra Super Crtitical (Usc) Power Plant.
4. J.C. Vaillant, B. Vandenberghe, B. Hahn, H. Heuser, C. Jochum, T/P23, 24, 911 and 92: New grades for advanced coal-fired power plants—Properties and experience. International Journal of Pressure Vessels and Piping 85 (2008) 38–46
5. Bani P. Mohanty and David A. Shores, Role of chlorides in hot corrosion of a cast Fe–Cr–Ni alloy. Part I: Experimental studies. Corrosion Science 46, pp2893–2907, (2004).
6. Horst Hack and Greg Stanko, Experimental Results for Fireside Corrosion Resistance of Advanced Materials in Ultra-Supercritical Coal-Fired Power Plants. Presented at the 32nd International Technical Conference on Coal Utilization & Fuel Systems, June 10 – 15, 2007, Clearwater, Florida, USA.
7. Robert A. Rapp, Hot Corrosion of materials: afluxing mechanism. Dep't Materials Sci. & Eng.The Ohio State University2041 College Road, Columbus, OH 43210. Corrosion science 44 (2002), pp209-221.
8. Subhash Kamal, R Jayaganthan and S Prakash, High temperature cyclic oxidation and hot corrosion behaviors of superalloys at

900°C, Bull. Mater. Sci., Vol. 33, No. 3, June 2010, pp. 299–306. © Indian Academy of Sciences.

9. Ravindra Kumar, V.K. Tewari and Satya Prakash, Oxidation behavior of base metal, weld metal and HAZ regions of SMAW. Journal of Alloys and Compounds 479 (2009), pp432– 435 Journal homepage: www.elsevier.com/locate/jallcom weldment in ASTM SA210 GrA1 steel.
10. LI Wei-jie, LIU Yong, WANG Yan, HAN Chao, TANG Hui-ping, hot corrosion behavior of Ni–16Cr–xAl based alloys in mixture of Na2SO4−NaCl at 600 °C. Trans. Nonferrous met soc. China21 (2011) 2617-2625. www.tnmsc.cn.
11. Jun Ma, Su Meng Jiang, Jun Gong, Chao Sun (2013), Hot corrosion properties of composite coatings in the presence of NaCl at 700 and 900°C. Corrosion Science 70 (2013) 29–36. Journal homepage: www.elsevier.com/cate/corsci.
12. F. Karimzadeh, M. Heiedarbeigy, A. Saatchi, Effect of heat treatment on corrosion behavior of Ti–6Al–4V alloy weldments.journalofmaterialsprocessingtechnology206 (2008), .journalhomepage:www.elsevier.com/locate/jmatprotec.
13. L.-C. Chen, C. Zhang, Z.-G. Yang, Effect of pre-oxidation on the hot corrosion of CoNiCrAlYRe alloy. Corrosion Science 53 (2011) 374–380. Journal homepage: www.elsevier.com/locate/corsci.
14. Horst Hack and Greg Stanko, Effects of fuel composition and temperature on fireside corrosion resistance of materials for advanced ultra-supercritical coal fired power plants. Energy materials, 2(2004), pp241-248.
15. High Temperature Corrosion and Materials Application (#05208G), Chapter 9 Hot Corrosion in Gas Turbines. Follow the site, www.asminternational.org.
16. R.E. Williford, C.F. Windisch Jr, R.H. Jones, In situ observations of the early stages of localized corrosion in Type 304 SS using the electrochemical atomic force microscope. Materials Science and Engineering A288 (2000) 54–60. www.elsevier.com:locate:msea.
17. J.M. Aquino, C.A. Della Rovere, S.E. Kuri, Intergranular corrosion susceptibility in super martensitic stainless steel weldments. Corrosion Science 51 (2009) pp2316–2323. Journal homepage: www.elsevier.com/locate/corsci.
18. Jian Cao, Yi Gong, Kai Zhu, Zhen-Guo Yang, Xiao-Ming Luo, Fu-Ming Gu, Microstructure and mechanical properties of dissimilar materials joints between T92 martensitic and S304H austenitic steels. Materials and Design 32 (2011) 2763–2770. Journal homepage: www.elsevier.com/locate/matdes.
19. Zahida Begum, A. Poonguzhali, Ranita Basu, C. Sudha, H. Shaikh, R.V. Subba Rao, Awanikumar Patil, R.K. Dayal, Studies of the tensile and corrosion fatigue behaviour of austenitic stainless steels. Corrosion Science 53 (2011) 1424–1432. Journal homepage: www.elsevier.com/locate/corsci.
20. Dasara V.Rathnamma and R. Nagarajan, surface chemical study of ―hot corrosion life prediction model for marinegas turbine blades and guide vanes‖.
21. Dr. Rama S. Koripelli, Dr. David C. Crowe, Dr. David N. French, and Jonathan Brand, the Role of Fireside Corrosion on Boiler Tube Failures, Part I. April 1, 2010.
22. Horst Hack and Greg Stanko, Update on Fireside Corrosion Resistance of Advanced Materials for Ultra-Supercritical Coal-Fired Power Plants. Presented at The 31st International Technical Conference On Coal Utilization & Fuel Systems.
23. Adnan Syed, fireside corrosion study of superheater materials in advance power plants. PhD Academic Year: 2008 – 2011.
24. Kaiju Yina, Shaoyu Qiua, Rui Tanga, Qiang Zhanga, Lefu Zhangb, Corrosion behavior of ferritic/martensitic steel P92 in supercritical water. J. of Supercritical Fluids 50 (2009) 235–239. Journal homepage: www.elsevier.com/locate/supflu.
25. Byeongsoo Lim, Bumjoon Kim, Moonhee Park, Sungjoon Won, Elevated temperature behavior of creep and fatigue in welded p92 steel. International Journal of Modern Physics B VkS% World Sripntific Vol. 17, Nos. 8 & 9 (2003) 1621-1626 VP www.worldscientmc.com © World Scientific Publishing Company.